May 1986 LRP 291/86

ADLER : A 2-D + 2-D QUASILINEAR CODE

S. Succi, K. Appert and J. Vaclavik

Paper presented at

8th EPS Conf. on Computational Physics - Computing in Plasma Physics

Eibsee, near Garmisch-Partenkirchen, F.R. Germany

May 13 to 16, 1986

ADLER : A 2-D + 2-D QUASILINEAR CODE

S. Succi, K. Appert and J. Vaclavik

Centre de Recherches en Physique des Plasmas
Association Euratom - Confédération Suisse
Ecole Polytechnique Fédérale de Lausanne
21, Av. des Bains, CH-1007 Lausanne / Switzerland

Abstract

ADLER (Anomalous Doppler Lausanne Electron Runaway), a 2-D+2-D finite element code recently developed at CRPP, Lausanne, is presented. This code is designed to investigate problems associated with lower-hybrid current drive. The basic structure of the code, including its convergence properties, is briefly illustrated together with some problems related to the discretization of the time variable, which arise in a long-time evolution.

Introduction

The remarkable progress recently made in the domain of lower hybrid current drive has provided a considerable impetus on the development of theoretical models describing the behaviour of the plasma under the effect of rf power and electric field [1]. Although a qualitative comprehension can be obtained with semi-analytical methods, it is nonetheless very important to try to parallel the experimental progress with a corresponding improvement of the numerical tools.

In this paper, we describe our new 2-D+2-D quasilinear code ADLER that simultaneously evolves the electron distribution function $f(v_\parallel, v_\perp, t)$ and the wave spectral distribution $W(k_\parallel, k_\perp, t)$ both in two dimensions.

Basic Equations

ADLER is devised to solve the following quasilinear equations:

$$\partial f/\partial t = (\hat{C} + \hat{Q} + \hat{E})f \qquad (1)$$

$$\partial W/\partial t = (2\gamma - \Sigma\nu_{ei}) + S \qquad (2)$$

with the initial conditions $f(\vec{v},o) = \phi(\vec{v})$ and $W(\vec{k},o) = W_o(\vec{k})$, where ϕ is an arbitrary function eventually modelling unstable situations and S represents an rf power source. The term $\hat{C}f$ is a linearized collision operator:

$$\hat{C}f = \frac{\nu_{ei}}{\omega_{pe}} \vec{\nabla}\cdot\left\{\frac{2\vec{v}}{v^3} f + \left[2\frac{\vec{v}\vec{v}}{v^5} + \frac{(1+Z)}{v}\left(\vec{\vec{I}} - \frac{\vec{v}\vec{v}}{v^2}\right)\right]\cdot\vec{\nabla}f\right\} \qquad (3)$$

where ν_{ei} is the electron-ion collision frequency, ω_{pe} the electron plasma frequency and Z the ion charge state. The term $\hat{Q}f$ stands for the quasilinear operator including both Cerenkov (n = o) and anomalous Doppler (n = 1) resonances:

$$\hat{Q}f = \sum_{n=0}^{1} \pi 2^{1-2n} \hat{L}_n \left[\int \left(\frac{k_\parallel}{k_\perp}\right)^2 \left(\frac{k_\perp v_\perp}{\omega_{ce}}\right)^{2n} \delta(\omega_n - k_\parallel v_\parallel) W(\vec{k},t) \frac{d_3\vec{k}}{(2\pi)^3}\right] \hat{L}_n f \qquad (4)$$

where $\hat{L}_n \equiv \partial/\partial v_\parallel - n(v_\parallel - k^{-1})v_\perp^{-1}\ \partial/\partial v_\perp$ and $\omega_n = k_\parallel/k + n\omega_{ce}$, ω_{ce} being the electron-cyclotron frequency. The symbol $\hat{E}f$ stands for the advective operator $\nu_{ei}/\omega_{pe}\ E\partial f/\partial v_\parallel$ which represents the inductive electric field. Finally, the quasilinear damping rate is given by $\gamma = \gamma_0 + \gamma_1$ with

$$\gamma_n = \pi 2^{-(2n+1)} \frac{k_\parallel^2}{k^3} \int \left(\frac{k_\perp v_\perp}{\omega_{ce}}\right)^2 \delta(\omega_n - k_\parallel v_\parallel) \hat{L}_n f\, d_3\vec{v} \qquad (5)$$

The normalizations adopted throughout the paper are :

$$k \to k/\lambda_D\ ,\ t \to t/\omega_{pe}\ ,\ v \to v v_{te}\ ,\ W \to W 4\pi n T \lambda_D^3\ ,\ E \to E m_e v_{te} \nu_{ei}/e$$

The Numerical Treatment

As a first step the unbounded $\vec{v}$ and $\vec{k}$ spaces are reduced to the corresponding finite size domains defined by:

$$\Omega = \left\{ V_1 \le v_\parallel \le V_2\ ;\ 0 \le v_\perp \le V_4 \right\}\ ;\ \Gamma = \left\{ K_1 \le k_\parallel \le K_2\ ;\ K_3 \le k_\perp \le K_4 \right\}$$

In these domains a finite element expansion of both the unknown functions f and W is adopted:

$$f = \sum_{i=1}^{N} f_i(t)\, \psi_i(v_\parallel, v_\perp) \qquad (6)$$

$$W = \sum_{\ell=1}^{M} W_\ell(t)\, \chi_\ell(k_\parallel, k_\perp) \qquad (7)$$

where the Ψ_i and χ_ℓ are bilinear and piecewise constant basis functions. The pivotal amplitudes $f_i(t)$, $W_\ell(t)$ become therefore

the actual unknowns of the problem. By inserting expressions (6) and (7) inequations (1) and (2) and subsequently projecting onto two sets of test functions ϕ_j and ξ_m respectively, we obtain a system of coupled O.D.E.s.

$$\sum_{J=1}^{N} a_{ij} \dot{f}_j = \sum_{J=1}^{N} \left(b_{ij}^{(0)} + \sum_{\ell=1}^{M} b_{ij\ell} W_\ell \right) f_j \tag{8}$$

$$\sum_{m=1}^{M} A_{\ell m} \dot{W}_m = \sum_{m=1}^{M} \left(B_{\ell m}^{(0)} + \sum_{J=1}^{N} B_{\ell m j}^{(1)} f_j \right) W_m + S_\ell \tag{9}$$

where $a_{ij} = \langle \phi_i | \Psi_j \rangle$, $A_{\ell m} = \langle \xi_\ell | \chi_m \rangle$ are the mass matrices.
The force matrices are given by :

$$b_{ij}^{(0)} = \langle \phi_i | \hat{C} + \hat{E} | \psi_j \rangle \tag{10}$$

$$b_{ij\ell}^{(1)} = \langle \phi_i | \hat{Q}\{\chi_\ell\} | \psi_j \rangle \tag{11}$$

$$B_{\ell m}^{(0)} = -\nu_{ei} \langle \xi_\ell | \chi_m \rangle \tag{12}$$

$$B_{\ell m j}^{(1)} = 2 \langle \xi_\ell | \gamma\{\psi_j\} | \chi_m \rangle \tag{13}$$

Here the bracket $\langle \bullet | \bullet \rangle$ stands for the usual scalar product in $L_2(\Omega)$ or $L_2(\mathbb{T})$. We note that the matrices $b^{(1)}$ and $B^{(1)}$ involve 4-dimensional integrations. However, since the Dirac operators only involve $v_\parallel$, the integration over $v_\perp$ can be singled out.

The treatment of the time variable is the same as in our previous codes [2]: A synchronous two-level scheme is adopted for the time discretization with an adjustable parameter which allows a transition between fully explicit and fully implicit schemes. The nonlinearity of the resulting equations is handled with a Picard scheme and the resulting algebraic problem is solved with a direct Gauss elimination technique at each time and iteration step.

Results

To date, the most severe validation tests for ADLER are made for the two-dimensional quasilinear beam relaxation. In this case, the particle density, the total momentum and energy are conserved and provide therefore a diagnostic tool for the numerical scheme. However, these conservation properties cannot be exactly translated into the numerical scheme. To see this, we write the rate of nonconservation of the parallel momentum $\Delta\dot{P}$ and energy $\Delta\dot{\mathcal{E}}$ in the form (only the most critical case of anomalous Doppler is considered) :

$$\Delta\dot{P} = \sum_{\ell,i=1}^{MN} P_{\ell i}\, W_\ell(t) f_i(t) \quad , \quad \Delta\dot{\mathcal{E}} = \sum_{\ell,i=1}^{N} \mathcal{E}_{\ell i}\, W_\ell(t) f_i(t)$$

where the matrices $P_{\ell i}$ and $\mathcal{E}_{\ell i}$ are expressed as :

$$P_{\ell i} \sim \iint (k_M - k)(k_\parallel/k^3)\, \chi_\ell\, \delta(v_\parallel - v_\parallel(\vec{k}))\, \hat{L}_1\, \psi_i\, d_3\vec{v}\, d_3\vec{k} \qquad (14)$$

$$\mathcal{E}_{\ell i} \sim \iint (v_{\parallel N} - v_\parallel)(k_\parallel/k^3)\, \chi_\ell\, \delta(v_\parallel - v_\parallel(\vec{k}))\, \hat{L}_1\, \psi_i\, d_3\vec{v}\, d_3\vec{k} \qquad (15)$$

where $k_M = \sum_{\ell=1}^{M} (|\vec{k}|)_\ell\, \chi_\ell$, $v_{\parallel N} = \frac{1}{2}\frac{d}{dv_\parallel} \sum_{i=1}^{N} (v_\parallel^2)_i\, \psi_i$

From these expressions we see that, for the conservation laws to hold exactly in the numerical scheme, the basis functions χ_ℓ and Ψ_i must represent exactly the functions $|\vec{k}| = \sqrt{k_\parallel^2+k_\perp^2}$ and v^2 respectively. In the present version χ_ℓ are piecewise constant and Ψ_i bilinear so that k_M and $v_{\parallel N}$ are both piecewise constant and consequently P_{il} and $\xi_{li} \neq 0$. In Fig. 1, the quantities $\Delta\dot{P}$, $\Delta\dot{\xi}$ at $t = 0$ are shown as functions of $\Delta k_\parallel \cdot \Delta k_\perp \equiv h^2$ for the case $V_1 = -4$, $V_2 = 8$, $V_4 = 5$ with 48×20 points in the $\vec{v}$ mesh and one cell in $\vec{k}$. As expected $\Delta\dot{P}$ decreases as $h^2 \to 0$, whereas $\Delta\dot{\xi}$ tends to a non-zero limit from below. This apparently strange behaviour is caused by the factor $v_{\parallel N}-v_\parallel$ whose sign is very sensitive to the location of the integration points $\vec{k}_g$ in the domain. If two different $\vec{k}_g$ are mapped symmetrically with respect to the mid-point of the interacting $v_\parallel$-cell, their contributions will exactly cancel one another. Normally $\vec{k}_g$ runs over a discrete set of uniformely distributed points, so that when h^2 increases many quasi-cancellations will occur. When $h^2 \to 0$, all $\vec{k}_g$ will be mapped on the same half-side of the $v_\parallel$-cell and their contributions must necessarily cumulate, leading to a higher error. This explanation is confirmed also by Fig. 2, where $\Delta\dot{\xi}$ and $\Delta\dot{P}$ are shown as functions of $\Delta v_\parallel \Delta v_\perp$ for a fixed value of $\Delta k_\parallel = \Delta k_\perp = 2 \times 10^{-4}$. The tendency of $\Delta\dot{\xi}$ to decrease with $\Delta v_\parallel \Delta v_\perp$ is a consequence of the fact that the single $\vec{k}_g$ contribution is roughly proportional to $\Delta v_\parallel$. The superimposed humped structure stems from the effects discussed above. The most effective remedy is therefore a rigid translation of the $v_\parallel$-grid which brings the mid-point $v_{i+1/2}$ as close as possible to $v_g = k_g^{-1} + \omega_{ce}k_{\parallel g}^{-1}$. For the present case ($v_g = 5.225$) by shifting the mesh from $(-4,8)$ to $(-3.9, 8.1)$ with 48×20 points one obtains a reduction of $\Delta\dot{\xi}$ of about three orders! Of course, the case just illustrated is a pedagogical one and in general it is very difficult to tailor the mesh in an optimal way for a realistic [1] domain. This means that there is a certain amount of non-conservation from the very beginning. Unfortunately, this situation worsens as the code evolves since at any time step further errors are introduced. This is clearly shown in Fig. 3, where the evolution of $|\Delta P|$ and $|\Delta\xi|$ is plotted for a realistic case: $V_1 = -4$, $V_2 = 16$, $V_4 = 15$, $K_1 = .04$, $K_2 = .4$, $K_3 = .04$, $K_4 = .2$ with a $60 \times 40 \times 30 \times 15$ mesh. From this figure we see that the relative nonconservation

increases with time. Unfortunately, iterating does not seem to help.

At present we are trying to improve this situation.

Acknowledgements

This work was partly supported by the Swiss National Science Foundation.

References:

[1] Comput. Phys. Commun. 40 (1986) No 1.

[2] Succi S. et al., Comput. Phys. Commun. 40 (1986) 137.

Figure Captions:

Fig. 1: The relative momentum and energy non conservation rates, $|\Delta\dot{P}/\dot{P}|$ and $|\Delta\dot{\mathcal{E}}/\dot{\mathcal{E}}|$ at t = 0, as functions of $\Delta k_{\parallel}\Delta k_{\perp}$ for $\Delta v_{\parallel} = \Delta v_{\perp} = 0.25$.

Fig. 2: The relative momentum and energy non conservation rates, $|\Delta\dot{P}/\dot{P}|$ and $|\Delta\dot{\mathcal{E}}/\dot{\mathcal{E}}|$ at t = 0, as functions of $\Delta v_{\parallel}\Delta v_{\perp}$ for $\Delta k_{\parallel} = \Delta k_{\perp} = 2 \times 10^{-4}$.

Fig. 3: The time evolution of the momentum and the energy non conservation $\Delta P, \Delta\mathcal{E}$ for the case $V_1 = -4$, $V_2 = 16$, $V_4 = 15$, $K_1 = 0.04$, $K_2 = 0.4$, $K_3 = 0.04$, $K_4 = 0.2$ with 60 intervals in $v_{\parallel}$, 40 in $v_{\perp}$, 30 in $k_{\parallel}$ and 15 in $k_{\perp}$.

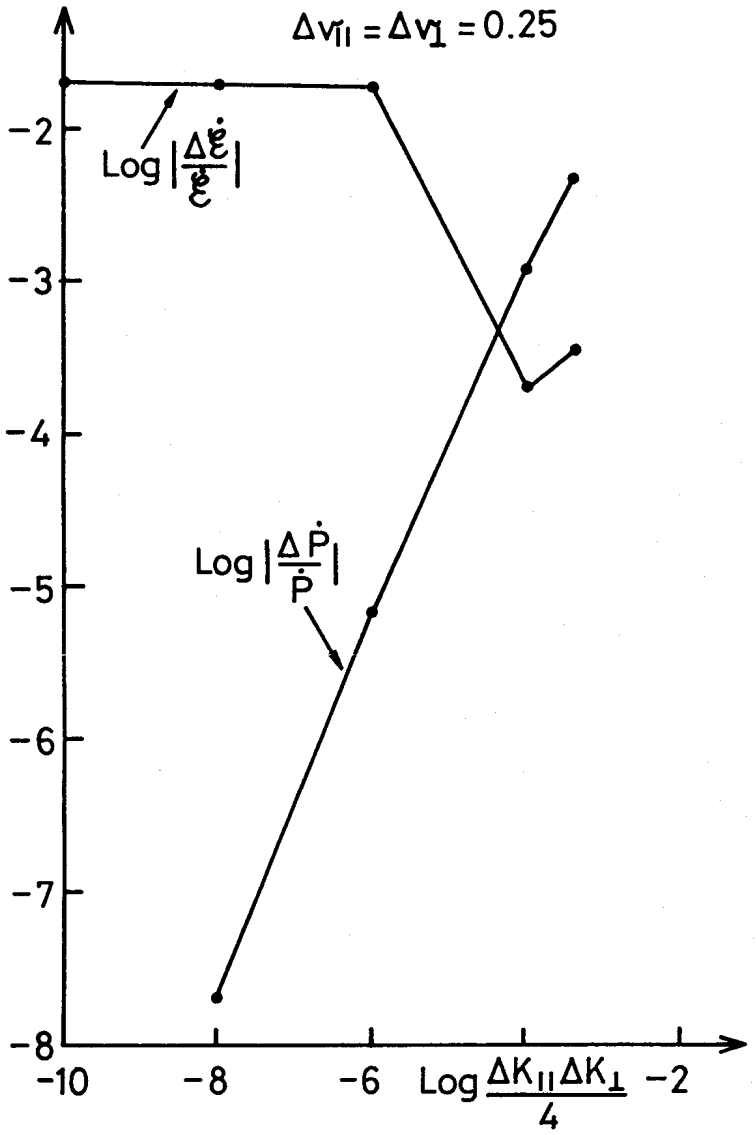
$\Delta\nu_{II} = \Delta\nu_{\perp} = 0.25$
$\text{Log}\left|\frac{\Delta\dot{\varepsilon}}{\dot{\varepsilon}}\right|$
$\text{Log}\left|\frac{\Delta\dot{P}}{\dot{P}}\right|$
-2
-3
-4
-5
-6
-7
-8
-10
-8
-6
$\text{Log}\frac{\Delta K_{II}\Delta K_{\perp}}{4}$
-2

Fig. 1

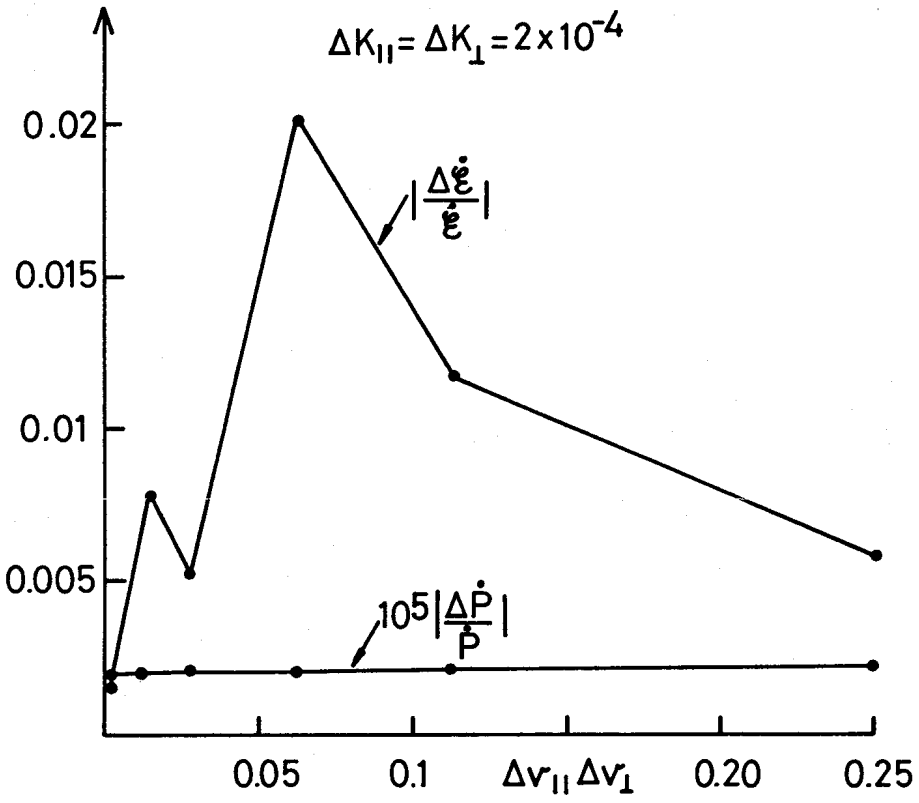
$\Delta K_{II} = \Delta K_{\perp} = 2\times10^{-4}$
$\left|\frac{\Delta\dot{\varepsilon}}{\dot{\varepsilon}}\right|$
$10^5\left|\frac{\Delta\dot{P}}{\dot{P}}\right|$
0.02
0.015
0.01
0.005
0.05
0.1
$\Delta\nu_{II}\,\Delta\nu_{\perp}$
0.20
0.25

Fig. 2

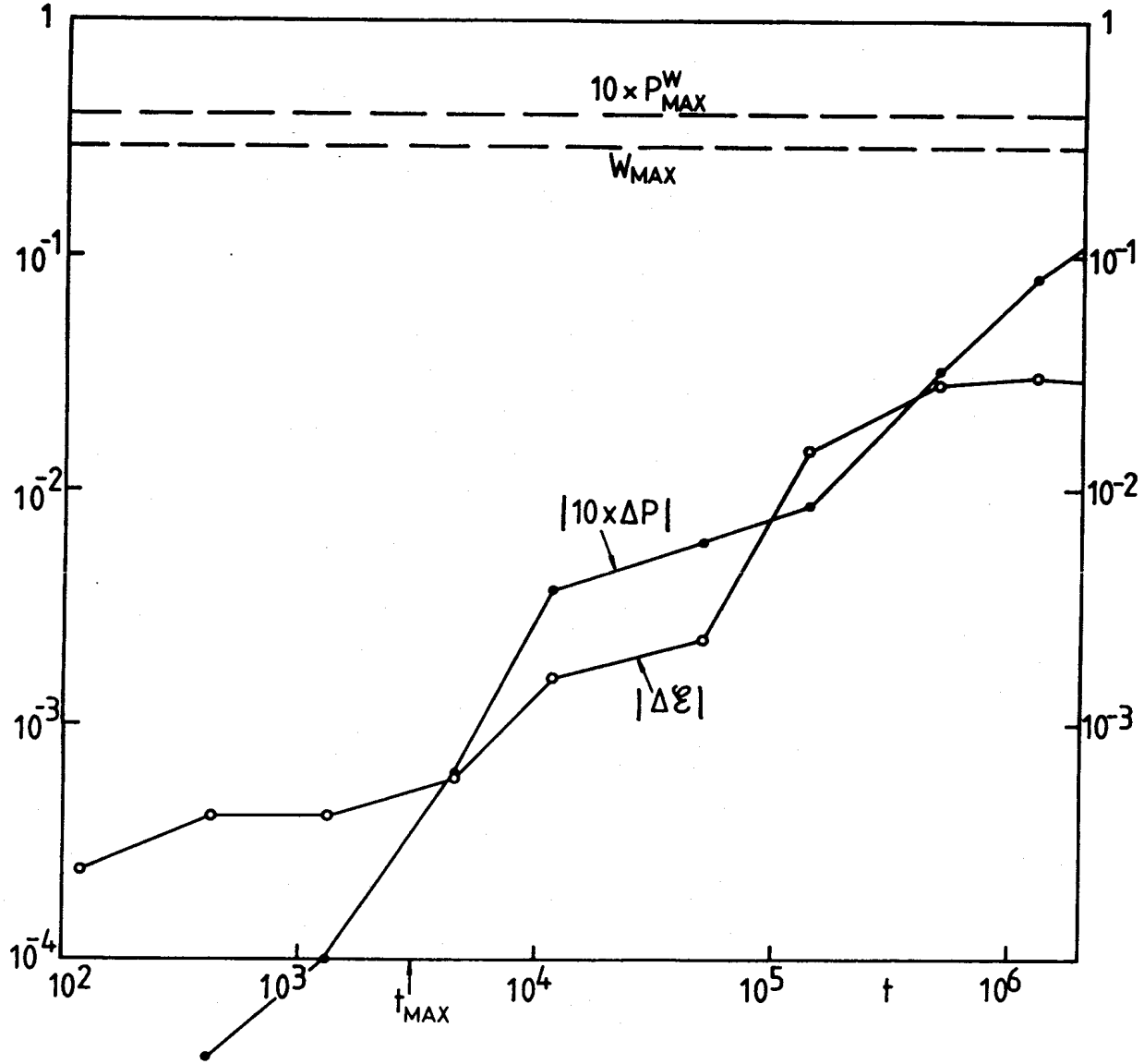
1
1
$10 \times P^{W}_{MAX}$
W_{MAX}
10^{-1}
10^{-1}
10^{-2}
10^{-2}
$|10 \times \Delta P|$
$|\Delta \mathcal{E}|$
10^{-3}
10^{-3}
10^{-4}
10^{2}
10^{3}
t_{MAX}
10^{4}
10^{5}
t
10^{6}

Fig. 3